NJC

Accepted Manuscript

This article can be cited before page numbers have been issued, to do this please use: S. Bahadorikhalili, M. Mahdavi, L. Ma'mani, A. Shafiee, H. Mahdavi and T. Akbarzadeh, *New J. Chem.*, 2018, DOI: 10.1039/C7NJ04837H.

ROYAL SOCIETY OF CHEMISTRY

rsc.li/njc

ROYAL SOCIETY OF CHEMISTRY
View Article Online
DOI: 10.1039/C7NJ04837H

Journal Name

ARTICLE

Palladium Functionalized Phosphinite Polyethyleneimine grafted Magnetic Silica Nanoparticles as an Efficient Catalyst for the Synthesis of Isoquinolino[1,2-*b*]quinazolin-8-ones

Received 00th January 20xx,
Accepted 00th January 20xx

DOI: 10.1039/x0xx00000x

www.rsc.org/

Saeed Bahadorikhalili[a], Mohammad Mahdavi[b], Leila Ma'mani[c], Abbas Shafiee[d], Hossein Mahdavi*[,a] and Tahmineh Akbarzadeh*[,d]

In this paper, a novel methodology is introduced for the synthesis of novel 5-methyl-8*H*-isoquinolino[1,2-*b*]quinazolin-8-one derivatives based on an efficient immobilized palladium catalyzed intramolecular carbon-carbon bond formation. The novel catalyst is fabricated by immobilization of Pd on phosphinite polyethyleneimine functionalized Fe_3O_4@SiO_2 core-shell nanoparticles (denoted as Pd@$OPPh_2$-PEI-mSiO_2 NPs). In this catalyst, PEI moieties act as both water dispersant and base in the reaction. In the key step, 3-allyl-2-(2-bromophenyl)-2,3-dihydroquinazolin-4(1*H*)-ones (3a-i) were synthesized via cyclization reaction between N-allyl-2-aminobenzamides and 2-bromobenzaldehyde. The latter obtained materials then underwent an intramolecular carbon-carbon bond formation in the presence of Pd@Ph_2PO-PEI-mSiO_2 catalyst to give 5-methyl-13,13a-dihydro-8*H*-isoquinolino[1,2-*b*]quinazolin-8-ones (4a-i).

Introduction

In the last few decades, transition metal-catalyzed carbon-carbon bond formation has proven to be one of the most direct and efficient methods for the preparation of complex chemical compounds.[1] Among different metals which are used as catalyst, palladium is an efficient one, which has attracted interests due to its unique properties. [2] Palladium catalysts are used in several organic transformations, especially in carbon-carbon bond formation reactions. [3] Mizoroki-Heck reaction is an important carbon-carbon bond formation reactions, which is catalyzed by palladium, and has intensely attracted interests in recent years. [4] Applying Mizoroki-Heck reaction in intramolecular carbon-carbon bond formation is a useful way for the synthesis of complex chemical compounds such as cyclic ketones, [5] 11-methyl-6*H*-isoindolo[2,1-*a*]indol-6-ones, [6] and substituted cycloheptenone dericvatives. [7]

Magnetic NPs have displayed high applicability in different fields including chemistry and catalysis [8] and known as effective research tools to improve novel and operative magnetically recoverable catalysts. [9] Their widespread usage and versatility make magnetic silica core-shell NPs excellent and interesting supporting materials for providing new and improved green catalysts. [9e] Regarding the great progress which has been achieved in the field of catalytic reactions, novel solid supported phosphine ligands have been used as a robust supporting material for the immobilization of transition metals and their applications as a catalyst in organic transformations. Regarding the unique properties of poly(ethyleneimine) (PEI) including physical and chemical stabilities, good water solubility, and high content of functional groups, it has attracted interest for the functionalization of nanoparticles. Covalent functionalization of nanoparticles by PEI has been successfully applied for directed drug delivery, gas adsorption and separation techniques, and as a support for immobilization of catalysts. [10]

Quinazolinone derivatives are probably the most ubiquitous nitrogen-containing heterocycles in nature and have been referred to as privileged scaffolds in drug discovery.[11] Their valuable properties, such as antitumor,[12] anticonvulsant,[13] anti-inflammatory, [14] and epidermal growth factor receptor (EGFR) tyrosine kinase inhibitory activities,[15] have attracted a great deal of attention. Also, they have been well known as peptidomimetic scaffold.[16] Among the various quinazolinones, isoquinolinone derivatives widely occur in natural products, [17] they are also versatile building blocks for the total synthesis of natural alkaloids.[18] Some isoquinolinones exhibit various biological and medicinal activities such as antihypertensive activity [19] and act as NK3 antagonists,[20] melatonin MT1 and MT2 receptor agonists,[21] Rho-kinase inhibitors, [22] and JNK

[a] *School of Chemistry, College of Science, University of Tehran, P. O. Box:14155-6455, Tehran, Iran*
[b] *Endocrinology Metabolism Research Center, Endocrinology Metabolism Clinical Sciences Institute, Tehran University of Medical Science, Tehran, Iran*
[c] *Department of Nanotechnology, Agricultural Biotechnology Research Institute of Iran (ABRII), Agricultural Research, Education and Extension Organization (AREEO), Karaj, Iran*
[d] *Department of Medicinal Chemistry, Faculty of Pharmacy ,Tehran University of Medical Sciences, Tehran, Iran*
Email: hmahdavi@khayam.ut.ac.ir, akbarzad@tums.ac.ir
† Footnotes relating to the title and/or authors should appear here.
Electronic Supplementary Information (ESI) available: [details of any supplementary information available should be included here]. See DOI: 10.1039/x0xx00000x

inhibitors.[23] They also are novel orally active 5-HT3 antagonists,[24] thymidylate synthase (TS) inhibitors,[25] or applied for the treatment of stomach tumors and diseases of human brain cells. [17b] Isoquinolino[1,2-*b*]quinazolin-8-ones derivatives shown cytotoxic activity. [17f]

Regarding our previous efforts on the synthesis of quinazolinone derivatives [26] on one hand, and extending methodologies based on Pd catalyzed reactions,[27] herein, we report a promising cyclization reaction methodology via an intramolecular Heck reaction using Pd catalyst decorated on phosphinite polyethyleneimine modified magnetic silica NPs to obtain novel 5-methyl-8*H*-isoquinolino[1,2-*b*]quinazolin-8-ones (4a-i) (Scheme 1).

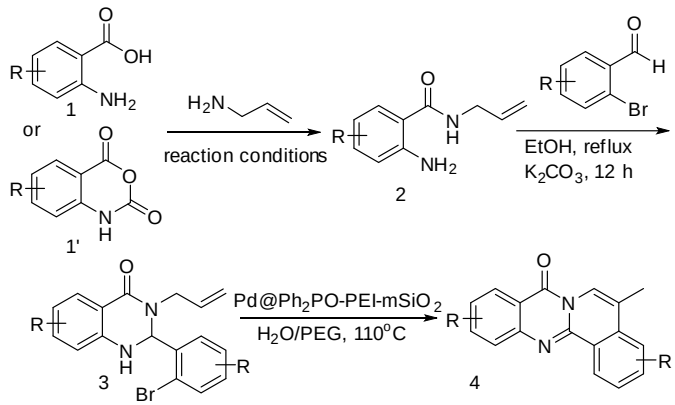

Scheme 1 Synthesis of 5-methyl-13,13a-dihydro-8*H*-isoquinolino[1,2-*b*]quinazolin-8-one derivatives (4a-i)

Results and Discussion

View Article Online
DOI: 10.1039/C7NJ04837H

To prepare the Pd catalyst based on modified magnetic NPs, superparamagnetic Fe_3O_4 NPs were initially synthesized and characterized according to our previous reported methods. [27c] Afterwards, to improve their stability and biocompatibility, the magnetic NPs were coated with silica shell generated by hydrolysis and condensation of TEOS to form magnetic Fe_3O_4@SiO_2 ($mSiO_2$) NPs. Then $mSiO_2$ was functionalized by decoration of the nanoparticle surface with PEI chains via the covalent grafting using PEI_{1200}–silane obtained from the treatment of PEI_{1200} and TESPIC. [27d] Introduction of PEI grafts onto the $mSiO_2$ NPs was both for the increasing the hydrophilicity of the catalyst, and application as a base in the reaction. In continuation, the PEI $mSiO_2$ NPs was treated with chlorodiphenylphosphine ($ClPPh_2$) to give the decorated phosphinite ligand on the surface of modified magnetic NPs. Finally, PEI phosphinite moiety was applied as a dispersible pendant for immobilizing of Pd NPs on the surface of $mSiO_2$ NPs. Therefore, as synthesized PEI-$OPPh_2$-$mSiO_2$ was reacted with $Pd(OAc)_2$ to provide Pd@Ph_2PO-PEI-$mSiO_2$ as the designed catalyst (Scheme 2). It is noticeable that the phosphinite group present in the structure of the catalyst acts as an efficient complexing agent for Pd(II). The structure of Pd@Ph_2PO-PEI-$mSiO_2$ was characterized by diverse techniques including high resolution transmission electron microscopy (HRTEM), vibrating sample magnetometer (VSM), thermal gravimetric analysis (TGA), Fourier transform infrared spectroscopy (FT-IR), N_2 adsorption–desorption analysis, and inductively couple plasma-atomic emission spectrometry (ICP-AES) analysis.

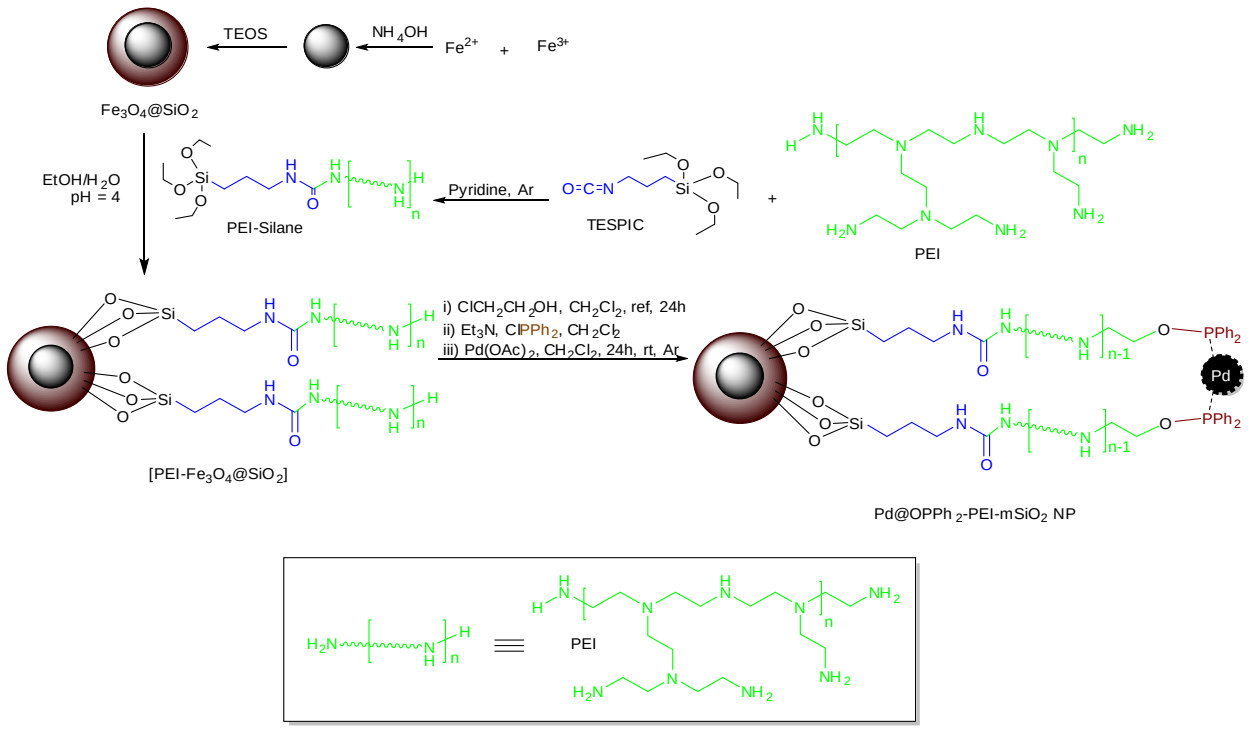

Scheme 2 The synthesis of Pd@$OPPh_2$-PEI-$mSiO_2$

View Article Online
DOI: 10.1039/C7NJ04837H

Journal Name

ARTICLE

For studying the structural morphology and core-shell structure of the Pd@Ph_2PO-PEI-mSiO_2, SEM and HRTEM images were applied. The TEM images of Pd@PEI-OPPh_2-mSiO_2 can be seen in **Fig. 1a** and **1b**. In the HRTEM image, the superparamagnetic Iron oxide nanoparticles can be seen as dark spots encapsulated by more bright silica shell. The more bright regions which are capsulated SPIONs are correlated to SiO_2 coating and the organic functionalization. The particles showed narrow dispersity with particles size between 20-25 nm. The core-shell structure can clearly be seen in the images. In SEM images, the spherical morphologies of the nanoparticles can clearly be observed.

The magnetic behavior of mSiO_2 NPs before and after post modifications, the magnetic hysteresis was assessed by VSM in an applied magnetic field at r.t, with the field sweeping from −8000 to +8000 Oe. The superparamagnetic nature of mSiO_2 and Pd@Ph_2PO-PEI-mSiO_2 has been shown by their S-type magnetization hysteresis loop (**Fig. 2a**). As illustrated in Fig. 2b, the images of aqueous solutions of Pd@Ph_2PO-PEI-mSiO_2 with and without external magnet firmly have demonstrated the sufficient magnetization for the magnetically separation.

TG analysis was applied to reveal the thermal stability and also to determine the amount of loaded PEI phosphinite on the surface of mSiO_2 NPs (**Fig. 3**). TGA curves confirm that Pd@Ph_2PO-PEI-mSiO_2 catalyst is thermally stable (up to 300°C) and shows no significant weight lose less than 300 °C. The TG curve of Ph_2PO-PEI-mSiO_2 and Pd@PEI-OPPh_2-mSiO_2 show a sharp decrease in weight was observed at 300 °C – 700 °C. Regarding the weight loss on TGA curves, the amount of loaded PEI phosphinite moiety determined 1.9 mmol IL g^{-1}.

In addition, the presence of PEI-phosphinite on the surface of magnetic nanoparticles was proved by TG analysis. We note that, the TG curve of mSiO_2 has no weight loss after 300 °C, but for Ph_2PO-PEI-mSiO_2 and Pd@Ph_2PO-PEI-mSiO_2 a sharp decrease in weight was observed at 300 °C – 700 °C, which can be attributed to the decomposition of the organic moieties grafted onto the surface of mSiO_2 (**Fig. 3**).

The surface area of the synthesized NPs was determined by Brunauer–Emmett–Teller (BET) theory. The large surface area of mSiO_2 magnetic nanoparticles was related to the small particle size of this material as could be observed in TEM images. Moreover, the content of the Pd in the catalyst was investigated by ICP-AES. the Pd content of the obtained catalyst was 0.82 mmol.g^{-1} in the Pd@Ph_2PO-PEI-mSiO_2 catalyst using ICP-AES.

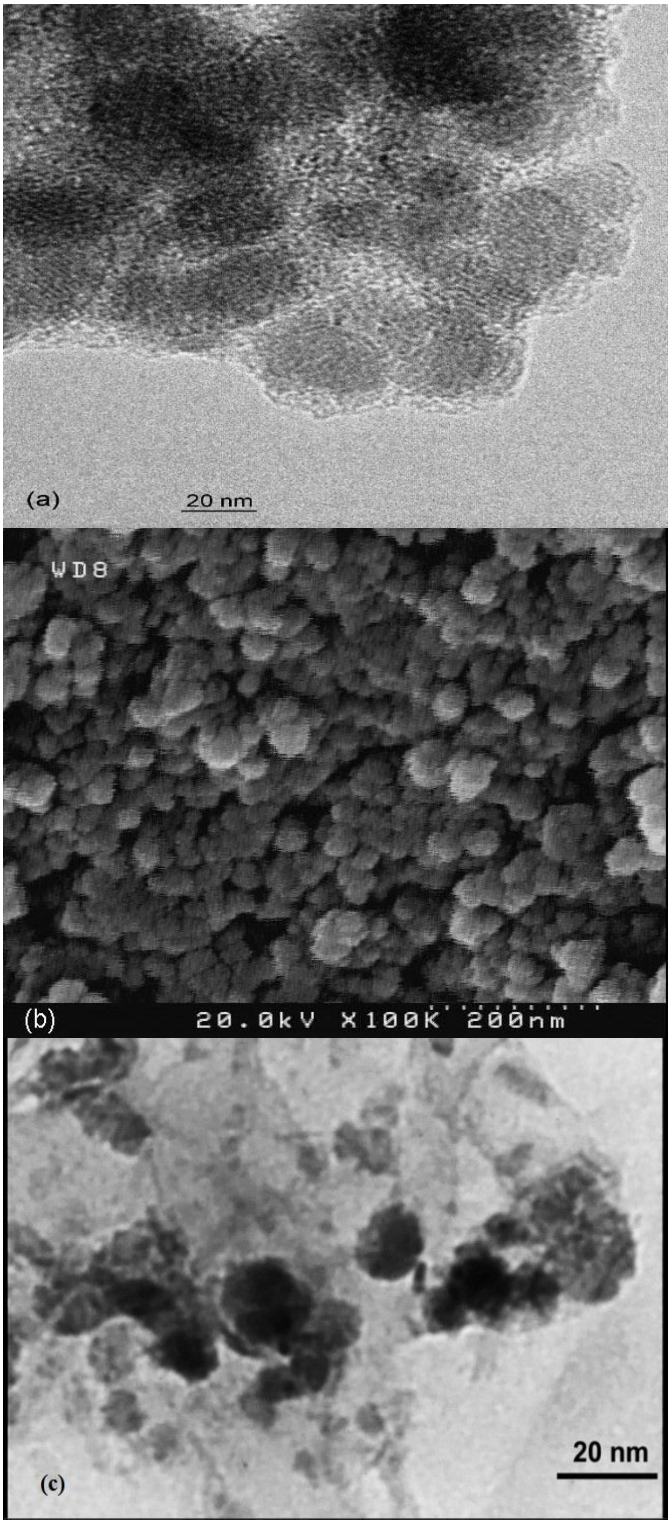

Figure 1 (a) HRTEM, (b) SEM and (c) TEM images of Pd@PEI-OPPh_2-mSiO_2

View Article Online
DOI: 10.1039/C7NJ04837H

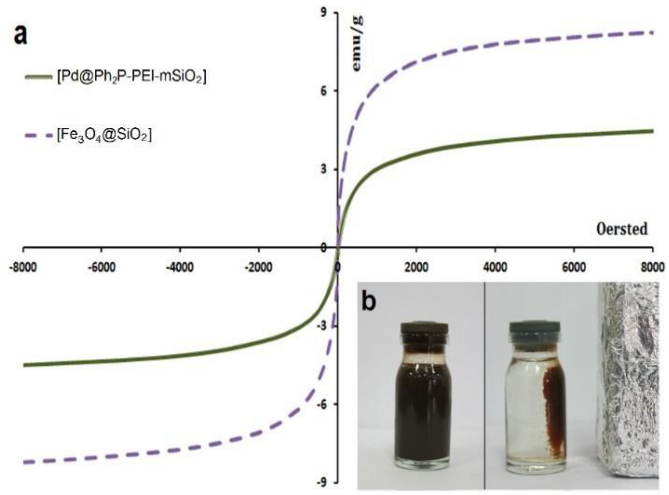

Figure2 (a) VSM diagram of $mSiO_2$ and $Pd@Ph_2PO\text{-}PEI\text{-}mSiO_2$; and (b) high water dispersion and facile magnetic separation of $Pd@Ph_2PO\text{-}PEI\text{-}mSiO_2$

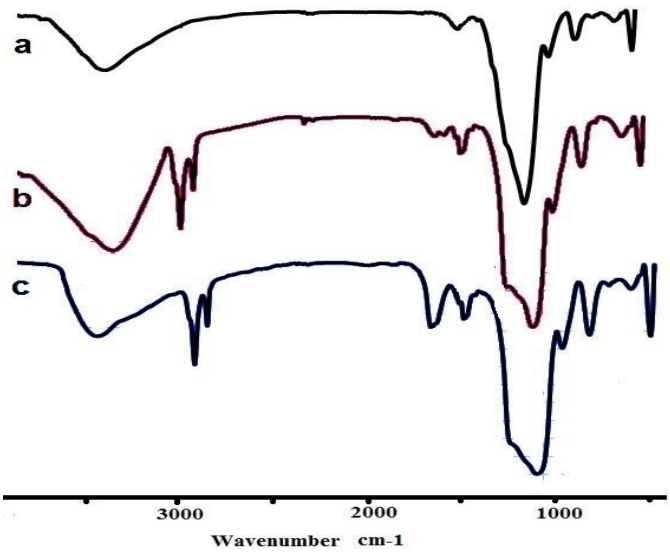

Figure 4 FTIR spectra for (a) $mSiO_2$, (b) $PEI\text{-}mSiO_2$, and (c) $Pd@Ph_2PO\text{-}PEI\text{-}mSiO_2$.

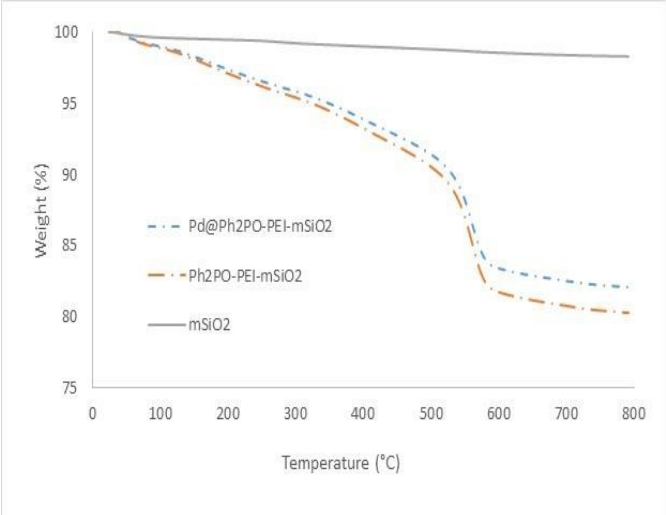

Figure 3. TG analysis of $mSiO_2$, $Ph_2PO\text{-}PEI\text{-}mSiO_2$, and $Pd@Ph_2PO\text{-}PEI\text{-}mSiO_2$ catalyst

FT-IR spectra of $mSiO_2$ NPs showed characterization peaks for Fe–O–Fe, Si–O–Si and O–H groups (Fig. 4a), which indicates the presence of iron oxide and silica phases. As shown in Fig 4b, after the reaction between PEI_{1200}–silane and $mSiO_2$, the resultant PEI $mSiO_2$ did not show any vibration at 2000–2500 cm^{-1} which confirmed the absence of the isocyanate group. Meanwhile, the successful immobilization of PEI phosphinite on the surface of $mSiO_2$ in $PEI\text{-}OPPh_2\text{-}mSiO_2$ catalyst was confirmed by additional peaks observed at 1677 cm^{-1} and 1491 cm^{-1} which could be assigned to C=O bonds (Fig. 4c).

We expected that the immobilization of PEI pincer-like phosphinite pendant on the surface of magnetic NPs provides a good distribution of catalytically active Pd species on the support and accordingly it stabilizes the Pd NPs during the chemical reaction, and also prevents the aggregation of Pd NPs. Therefore, PEI plays multiple role in giving more hydrophilic character to the catalyst and acting as base during the reaction.

The activity of the catalyst was subsequently investigated upon characterization in the intramolecular Heck reaction. The reaction was studied for finding the optimized conditions. Blank runs with provided the lack of catalytic activity in the presence of $mSiO_2$ or $Ph_2PO\text{-}PEI\text{-}mSiO_2$ NPs as catalyst. The performance of the reaction showed to be independent to in the presence of a base beside the catalyst. Therefore a series of bases including NaOH, KOH, K_2CO_3, pyridine and NEt_3 were screened. The great advantage of pendant PEI groups is their role as base in the reaction (Table 1, Entry 1). In addition the catalytic activity of the $Pd@Ph_2PO\text{-}PEI\text{-}mSiO_2$ was compared with non-immobilized palladium catalyst (Table 1, Entries 7-14). For this purpose, palladium acetate (Table 1, Entries 7-10) and palladium chloride (Table 1, Entries 11-14) were used as catalyst for the synthesis of the desired products. As can be seen, the desired products have been obtained when non-immobilized palladium salts are applied as catalyst in a very lower yields.

Then the effect of the amount of the catalyst on the reaction was investigated and different quantities of catalyst ranging from 0.001 to 0.050 g were tested. The best results were observed when 0.015 g of the catalyst (0.82 mmol of Pd in each gram of the catalyst) has been applied, while using more quantities of the catalyst did not improve the reaction performance. we note that in the absence of the catalyst, no product was formed, which proves that, the presence of the catalyst is necessary for the reaction. However, the performance of the reaction was investigated in the presence of $PEI\text{-}mSiO_2$ nanoparticles without any palladium loading. Also in this case, no product could be formed. This observation proves that, $PEI\text{-}mSiO_2$ without palladium nanoparticles do not show any catalytic activity in this reaction.

For comparing the catalytic activity of $Pd@Ph_2PO\text{-}PEI\text{-}mSiO_2$ with other palladium catalysts, the reaction was performed in $Pd(OAc)_2$, $PdCl_2$ and Pd-PVP catalyst (Table 1, Entries 7-18).[4d,4e] As can be seen in Table 1, the desired product is obtained in all cases. But the isolated yields were lower than $Pd@Ph_2PO\text{-}PEI\text{-}mSiO_2$ catalyzed reactions.

Table 1 Effect of different based on the reaction time and the isolated yield [a]

Entry	Base	Catalyst (g)	Time (h)	Yield (%)
1	---	$Pd@Ph_2PO$-PEI-$mSiO_2$ [b]	24	83
2	DIPEA	$Pd@Ph_2PO$-PEI-$mSiO_2$	36	62
3	KOH	$Pd@Ph_2PO$-PEI-$mSiO_2$	36	58
4	K_2CO_3	$Pd@Ph_2PO$-PEI-$mSiO_2$	48	67
5	pyridine	$Pd@Ph_2PO$-PEI-$mSiO_2$	48	75
6	NEt_3	$Pd@Ph_2PO$-PEI-$mSiO_2$	48	71
7	NaOH	$Pd(OAc)_2$ [c]	48	66
8	pyridine	$Pd(OAc)_2$	48	71
9	DIPEA	$Pd(OAc)_2$	48	64
10	K_2CO_3	$Pd(OAc)_2$	48	59
12	NaOH	$PdCl_2$ [c]	48	56
13	pyridine	$PdCl_2$	48	75
14	DIPEA	$PdCl_2$	48	72
15	K_2CO_3	Pd-PVP [d]	36	71
16	NaOH	Pd-PVP	36	67
17	pyridine	Pd-PVP	36	69
18	DIPEA	Pd-PVP	36	66

[a] Reaction conditions: 3 (1 mmol), H_2O:PEG (5 mL), and base (1.5 eq) at 110°C; [b] $Pd@Ph_2PO$-PEI-$mSiO_2$ catalyst (0.82 mmol of Pd in each gram of the catalyst); [c] $Pd(OAc)_2$ or $PdCl_2$ (5 mol %), PPh_3 (10 mol%), PEG (5 mL), and base (1.5 eq) at 110 °C; [d] Pd-PVP (5 mol%), H_2O:PEG (5 mL), and base (1.5 eq) at 110 °C.

Afterwards, the performance of the reaction was studied in different solvents. As can be seen in table 2, the synthesis of 5-methyl-13,13a-dihydro -8*H*-isoquinolino[1,2-*b*]quinazolin-8-one derivatives was performed in different protic and aprotic solvents with different polarities. The results show that, a 50:50 (v/v) mixture of H_2O/PEG_{600}. Finally, performing the reaction in different temperature conditions proved 110°C as the best one for yielding the desired product.

Table 2 Effect of different solvents on the reaction time and the yield [a]

Entry	Solvent	Time (h)	Isolated Yield (%)
1	H^2O	47	41
2	DMF	36	56
3	DMSO	36	62
4	PEG/H^2O [b]	24	83
5	EtOH	48	48
6	CH_2Cl_2	48	55
7	CH_3CN	48	41

[a] Reaction conditions: 3 (1 mmol), solvent (5 mL), and catalyst (0.015 g) at 110°C; [b] 50:50 (v/v) mixture

Having the optimized conditions in hand, the scope of the Pd catalyzed intramolecular cyclization reactions of 3-allyl-2-(2-bromophenyl)-2,3-dihydroquinazolin-4(1*H*)-ones (3a-i) was investigated. As shown in Table 3, $Pd@Ph_2PO$-PEI-$mSiO_2$ successfully catalyzes the reaction to give the desired products. The corresponding 5-methyl-13,13a-dihydro-8*H*-isoquinolino[1,2-*b*]quinazolin-8-one derivatives (4a-i) were obtained in moderate to good yields for various examined substrates at 110 °C. As illustrated, a wide range of isoquinazolinone can be efficiently produced with this catalytic system. All substrates possessing electron-rich as well as electron-poor substituents underwent intramolecular cyclization catalyzed by $Pd@Ph_2PO$-PEI-$mSiO_2$. Starting materials containing heteroatoms were also performed the reaction (Table 3, 4e and 4f). It was noteworthy that the hetero-atoms could be tolerated under identical conditions with good yields.

Table 3 The synthesis of 5-methyl-13,13a-dihydro-8*H*-isoquinolino[1,2-*b*]quinazolin-8-one derivatives using $Pd@Ph_2PO$-PEI-$mSiO_2$ catalyst

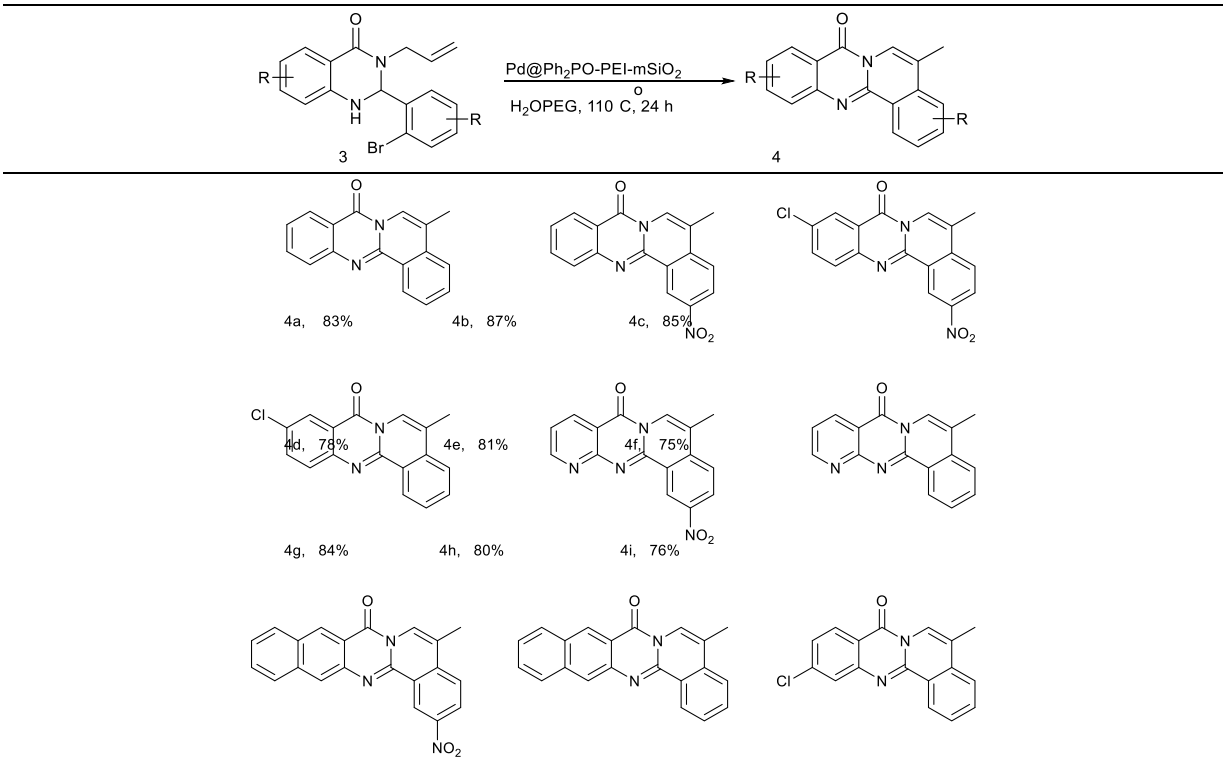

The reaction conditions: 3 (1 mmol), Pd@PEI-OPPh2-$mSiO_2$ (0.015 g, 0.82 mmol of Pd in each gram of the catalyst) and H_2O/PEG600 50:50 v/v (5 mL) at 110°C.

View Article Online
DOI: 10.1039/C7NJ04837H

Journal Name

ARTICLE

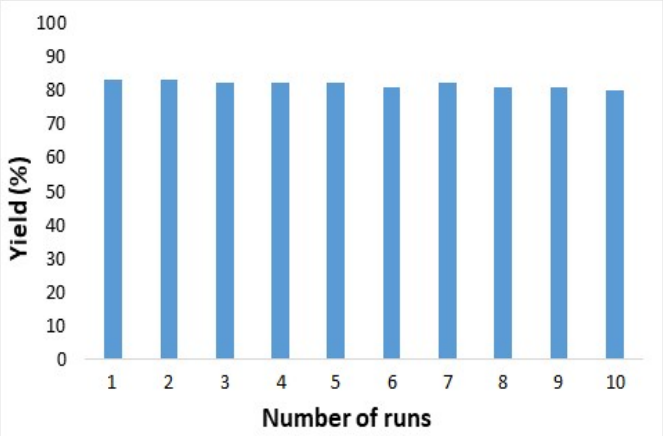

Figure 5 Reusability of Pd@Ph_2PO-PEI-$mSiO_2$ in the synthesis of triazolylquinazolinone after 10 runs

An advantage of current catalyst is its high reusability. The recycling of Pd@Ph_2PO-PEI-$mSiO_2$ catalyst tested in 10 sequential reactions for the preparation reaction of 5-methyl-8*H*-isoquinolino[1,2-*b*]quinazolin-8-one. The results are presented in Figure 5. It is obvious in Figure 5 that, no significant loss in the catalyst activity can be observed after 10th run. It can be due to the high stability of the catalyst, and low leaching of copper, which makes the structure of Pd@Ph_2PO-PEI-$mSiO_2$ catalyst stable during the reaction.

Experimental Section

Preparation of PEI Functionalized-Fe_3O_4@SiO_2

PEI_{1200}–silane was synthesized via the hydrogen-transfer nucleophilic addition reaction between PEI (MW = 1200) and the isocyanate group of 3-(triethoxysilyl) propyl isocyanate (TESPIC).[27d] First 0.01 mol of dried PEI_{1200} was dissolved into 50 mL of dry pyridine with vigorous stirring under argon atmosphere for 6 h at 70 °C, and then, 0.01 mol of TESPIC was added. After more 24 h stirring of the reactioin mixture, the solvent was removed by vacuum evaporation and the residue was washed three times with *n*-hexane. The obtained white PEI_{1200}–silane was filtered at 0 °C and then dried at room temperature in vacuum.
Then a solution of 0.1 g of PEI_{1200}–silane in 30 mL of EtOH was added drop-wise to a vigorous stirring solution of 25 mg of Fe_3O_4@SiO_2 nanoparticles, which was prepared according to the reported procedure, [8d] in 30 mL EtOH/H_2O (1:2) and HCl (pH = 4). After vigorous stirring for 24 h, the solution was filtered off and washed thoroughly. The white residue was dried at 100 °C in vacuum for 12 h to obtain PEI-$mSiO_2$.

Preparation of ethanol modified PEI-Fe_3O_4@SiO_2

2-chloroethanol (0.4 g, 5 mmol) was poured to a mixture of PEI-$mSiO_2$ (2 g) in 50 ml toluene and the mixture was stirred at 90 °C overnight. Then the solid residue was magnetically separated, washed with toluene and Et_2O, and dried in a vacuum oven at 50 °C for 24 h. The dried magnetic solid (2 g) and triethylamine (0.505 g, 5 mmol) were added to a solution of chlorodiphenylphosphine (1.1 g, 5 mmol) in dry CH_2Cl_2. The mixture was stirred under argon atmosphere for 12 h at room temperature. Then the solid residue separated by a magnet, washed with CH_2Cl_2 and dried in a vacuum oven at 50 °C for 12 h to give Ph_2PO-PEI-$mSiO_2$.

Preparation of Pd@Ph_2PO-PEI-$mSiO_2$ catalyst

To a mixture of Ph_2PO-PEI-$mSiO_2$ (1 g) in 50 ml dry CH_2Cl_2, palladium acetate (2 mmol) was added and stirred at room temperature under argon atmosphere for 24 h. The obtained solid was magnetically separated and washed with CH_2Cl_2 (2×10 ml) and Et_2O (2×10 ml). Ph_2PO-PEI-$mSiO_2$ catalyst was obtained as a dark brown powder after drying under vacuum for 12 h.

General procedure for the preparation of *N*-allyl-2-aminobenzamide (2) from isatoic anhydrides

Isatoic anhydride (5 mmol) was poured in water (100 ml) and allylamine (6 mmol) was added dropwise during 30 min. The mixture was stirred overnight at room temperature. *N*-allyl-2-aminobenzamide product was formed as cream colored precipitates. The product was filtrated and washed 3 times with cold water and dried at room temperature. Typical yield for the products were above 95%.

General procedure for the preparation of *N*-allyl-2-aminobenzamide (2) from anthranilic acid

Anthranilic acid (1 mmol) was dissolved in dry dichloromethane. To this, Hydroxybenzotriazole (1.1 mmol) and allyl amine (1 mmol) was added. Following this, 1 equivalent of diisopropyl carbadiimide was added to the mixture and the reaction was mixed overnight. Upon completion of the reaction, the isopropyl urea was filtrated away and dichloromethane layer was washed with saturated sodium bicarbonate solution and then with 2M HCl. The organic layer was dried over anhydrous sodium sulfate and the solvent was then removed under reducer pressure. Typical yield for the products were above 80%.

General procedure for the synthesis of 3-allyl-2-(2-bromophenyl)-2,3-dihydroquinazolin-4(1*H*)-one derivatives (3)

N-allyl-2-aminobenzamide (3.0 mmol) and 2-bromobenzaldehyde (3 mmol) and K_2CO_3 (1.1 eqivalent) was dissolved in ethanol (20 ml) in a round flask equipped with condenser, heater and magnetic stirrer. The reaction mixture was refluxed for 24 h, while the reaction progress monitored by TLC. After completion of the reaction, the solvent was evaporated under reduced pressure and the product was recrystallized in ethanol to obtain pure product.

General procedure for Pd@Ph_2PO-PEI-$mSiO_2$ catalyzed intramolecular coupling of 3-allyl-2-(2-bromophenyl)-2,3-dihydroquinazolin-4(1*H*)-one derivatives to 5-methyl-8*H*-isoquinolino[1,2-*b*]quinazolin-8-ones

In a 1:1 mixture of H_2O:PEG_{600} (2 ml), 3-allyl-2-(2-bromophenyl)-2,3-dihydroquinazolin-4(1*H*)-one (1 mmol), sodium acetate (1.2 equivalent) and Pd@Ph_2PO-PEI-$mSiO_2$ (0.015 g) was added. The mixture was stirred at 90°C. TLC monitoring showed the reaction completion after 48 h. After completion of the reaction, the mixture was cooled to the room temperature and was poured into water (10 ml) and the product was extracted with ethyl

acetate. The organic phase was dried over Na_2SO_4. Then the combined organic phase was evaporated and the products were purified by column chromatography on silica gel using a mixture of *n*-hexane:ethyl acetate (5:1) as eluent. The recovered catalyst was rinsed with water and EtOH, and finally dried at r.t. and used without any pretreatment for the next run. The recycling test of the catalyst was performed in the reaction between bromobenzene and n-butyl acrylate according to the above procedure.

Spectral data of 3-allyl-2-(2-bromophenyl)-2,3-dihydroquinazolin-4(1*H*)-one derivatives

5-methyl-8*H*-isoquinolino[1,2-*b*]quinazolin-8-one (4a)

Yield: 83%; white crystals; mp 202-205°C (Lit. 203-205°C [17f]); Anal. Calcd for $C_{17}H_{12}N_2O$: C: 78.44, H: 4.65, N: 10.76, O: 6.15, Found: C: 78.28, H: 4.81, N: 10.89, O: 6.02; IR (KBr): υ = 1676, 1590 cm^{-1}; ^1H NMR (DMSO-d_6, 500 MHz): δ = 2.00 (3H, d, J = 1.5 Hz), 7.28-7.31 (3H, m), 7.35-7.38 (2H, m), 7.48-7.50 (1H, m), 7.69 (1H, q, J = 8.5 Hz), 7.82 (1H, d, J = 8.5 Hz), 8.01 (1H, s) ppm; ^{13}C NMR (DMSO-d_6, 125 MHz): δ = 23.1, 112.6, 117.3, 117.4, 121.6, 125.3, 127.1, 128.3, 129.4, 130.8, 132.5, 133.2, 138.0, 138.3, 146.5, 156.7, 161.0 ppm; MS (70 eV): m/z = 261 (M^+).

5-methyl-2-nitro-8*H*-isoquinolino[1,2-*b*]quinazolin-8-one (4b)

Yield: 87%; white crystals; mp 222-224°C (Lit. 224-226°C [17f]); Anal. Calcd for $C_{17}H_{11}N_3O_3$: C: 66.88, H: 3.63, N: 13.76, O: 15.72, Found: C: 67.12, H: 3.47, N: 13.57, O: 15.93; IR (KBr): υ = 1671, 1597 cm^{-1}; ^1H NMR (DMSO-d_6, 500 MHz): δ = 1.92 (3H, s), 6.82 (1H, s), 6.87 (1H, d, J = 8 Hz), 7.00 (1H, d, J = 7 Hz), 7.10-7.12 (1H, m), 7.15-7.20 (2H, m), 7.68 (1H, d, J = 1.5 Hz), 8.13 (1H, d, J = 7 Hz) ppm; ^{13}C NMR (DMSO-d_6, 125 MHz): δ = 21.6, 114.4, 115.6, 116.6, 116.9, 118.7, 121.9, 126.0, 126.2, 127.3, 129.3, 133.0, 133.3, 139.2, 146.5, 154.5, 162.3 ppm; MS (70 eV): m/z = 305 (M^+).

10-chloro-5-methyl-2-nitro-8*H*-isoquinolino[1,2-*b*]quinazolin-8-one (4c)

Yield: 85%; white crystals; mp 277-280°C (Lit. 279-281°C [17f]); Anal. Calcd for $C_{17}H_{10}ClN_3O_3$: C: 60.10, H: 2.97, N: 12.37, O: 14.13, Found: C: 60.24, H: 2.75, N: 12.22, O: 14.35; IR (KBr): υ = 1601, 1583, 1527 cm^{-1}; ^1H NMR (DMSO-d_6, 500 MHz): δ = 1.99 (3H, s), 7.22 (1H, s), 7.35 (1H, d, J = 8 Hz), 7.51 (1H, s), 7.65 (1H, d, J = 8 Hz), 7.97 (1H, d, J = 8 Hz), 8.33 (1H, d, J = 8 Hz), 8.54 (1H, s) ppm; ^{13}C NMR (DMSO-d_6, 125 MHz): δ = 18.3, 119.5, 121.9, 126.2, 127.0, 127.8, 128.1, 128.3, 128.4, 129.6, 129.7, 134.8, 136.3, 137.4, 145.9, 146.5, 160.3 ppm; MS (70 eV): m/z = 339 (M^+).

10-chloro-5-methyl-8*H*-isoquinolino[1,2-*b*]quinazolin-8-one (4d)

Yield: 78%; white crystals; mp 216-218°C (Lit. 217-219°C [17f]); Anal. Calcd for $C_{17}H_{11}ClN_2O$: C: 69.28, H: 3.76, N: 9.59, O: 5.43, Found: C: 69.54, H: 3.58, N: 9.81, O: 5.13; IR (KBr): υ = 1676, 1594cm^{-1}; ^1H NMR (DMSO-d_6, 500 MHz): δ = 1.93 (3H, s), 6.99 (1H, d, J = 9 Hz), 7.04 (1H, s), 7.29-7.36 (2H, m), 7.47 (1H, d, J = 7 Hz), 7.51 (1H, d, J = 9 Hz), 7.66-7.68 (2H, m), 8.16 (1H, s) ppm; ^{13}C NMR (DMSO-d_6, 125 MHz): δ = 19.2, 107.7, 113.5, 117.3, 117.5, 127.2, 128.4, 129.4, 132.6, 133.3, 136.3, 138.0, 139.2, 143.2, 145.5 157.1, 166.8 ppm; MS (70 eV): m/z = 294 (M^+).

5-methyl-2-nitro-8*H*-pyrido[2',3':4,5]pyrimido[2,1-*a*]isoquinolin-8-one (4e)

Yield: 81%; white crystals; mp 177-179°C; Anal. Calcd for $C_{16}H_{10}N_4O_3$: C: 62.74, H: 3.29, N: 18.29, O: 15.67, Found: C: 62.97, H: 3.44, N: 18.04, O: 15.53; IR (KBr): υ = 1685, 1582 cm^{-1}; ^1H NMR (DMSO-d_6, 500 MHz): δ = 1.99 (3H, s), 7.95 (1H, s), 8.13-8.19 (2H, m), 8.31-8.42 (2H, m), 7.58 (1H, t, J = 6 Hz), 8.92 (1H, s) ppm; ^{13}C NMR (DMSO-d_6, 125 MHz): δ = 20.3, 127.4, 128.1, 128.9, 130.2, 130.4, 130.5, 131.0, 131.1, 132.7, 134.7, 135.1, 137.6, 146.7, 153.5, 161.3 ppm; MS (70 eV): m/z = 306 (M^+).

5-methyl-8*H*-pyrido[2',3':4,5]pyrimido[2,1-*a*]isoquinolin-8-one (4f)

View Article Online DOI: 10.1039/C7NJ04835H

Yield: 75%; white crystals; mp 155-158°C; Anal. Calcd for $C_{16}H_{11}N_3O$: C: 73.55, H: 4.24, N: 16.08, O: 6.12, Found: C: 73.14, H: 4.55, N: 16.27, O: 5.92; IR (KBr): υ = 1676, 1606 cm^{-1}; ^1H NMR (DMSO-d_6, 500 MHz): δ = 2.51 (3H, s), 6.98 (1H, d, J = 8 Hz), 7.26-7.28 (2H, m), 7.50 (1H, s), 7.60 (1H, t, J = 8 Hz), 7.71 (1H, d, J = 8 Hz), 7.88 (1H, t, J = 8 Hz), 8.21 (1H, d, J = 8 Hz) ppm; ^{13}C NMR (DMSO-d_6, 125 MHz): δ = 20.9, 117.4, 118.8, 120.3, 126.4, 127.3, 128.2, 128.3, 129.8, 131.8, 133.7, 134.6, 134.7, 135.5, 146.8, 154.9, 161.3 ppm; MS (70 eV): m/z = 261 (M^+).

5-methyl-2-nitro-8*H*-benzo[*g*]isoquinolino[1,2-*b*]quinazolin-8-one (4g)

Yield: 84%; white crystals; mp 187-189°C; Anal. Calcd for $C_{21}H_{13}N_3O_3$: C: 70.98, H: 3.69, N: 11.83, O: 13.51, Found: C: 70.32, H: 3.45, N: 12.01, O: 13.23; IR (KBr): υ = 1679, 1590 cm^{-1}; ^1H NMR (DMSO-d_6, 500 MHz): δ = 2.00 (3H, d, 1.2 Hz), 7.26 (1H, t, J = 8.5 Hz), 7.32 (1H, t, 8.5 Hz), 7.56 (1H, d, 6 Hz), 7.66 (1H, s), 7.76 (1H, d, J = 8.5 Hz), 7.80 (1H, d, J = 8.5 Hz), 7.89 (1H, d, J = 6 Hz), 8.01 (1H, d, J = 8.5 Hz), 8.11 (1H, s), 8.42 (1H, s), 8.73 (1H, s) ppm; ^{13}C NMR (DMSO-d_6, 125 MHz): δ = 45.6, 115.1, 115.9, 116.3, 116.5, 117.3, 118.2, 118.4, 119.7, 122.3, 123.4, 125.3, 127.3, 129.0, 129.4, 141.1, 142.6, 149.7, 150.5, 160.2 ppm; MS (70 eV): m/z = 355 (M^+).

5-methyl-8*H*-benzo[*g*]isoquinolino[1,2-*b*]quinazolin-8-one (4h)

Yield: 80%; white crystals; mp 179-181°C; Anal. Calcd for $C_{21}H_{14}N_2O$: C: 81.27, H: 4.55, N: 9.03, O: 5.16, Found: C: 81.55, H: 4.77, N: 9.52, O: 5.95; IR (KBr): υ = 1675, 1588 cm^{-1}; ^1H NMR (DMSO-d_6, 500 MHz): δ = 2.02 (3H, d, J = 1 Hz), 7.14-7.22 (2H, m), 7.32-7.37 (2H, m), 7.41-7.49 (2H, m), 7.60-7.69 (2H, m), 7.91 (1H, d, J = 7 Hz), 8.27 (1H, s), 8.24 (1H, s) ppm; ^{13}C NMR (DMSO-d_6, 125 MHz): δ = 15.8, 109.1, 117.5, 120.1, 120.4, 121.5, 123.7, 124.8, 125.2, 126.8, 128.1, 128.9, 129.6, 130.7, 132.9, 136.4, 136.8, 143.5, 147.1, 153.7, 162.5 ppm; MS (70 eV): m/z = 310 (M^+).

11-chloro-5-methyl-8*H*-isoquinolino[1,2-*b*]quinazolin-8-one (4i)

Yield: 76%; white crystals; mp 183-185 °C; Anal. Calcd for $C_{17}H_{11}ClN_2O$: C: 69.28, H: 3.76, N: 9.50, O: 5.43, Found: C: 69.14, H: 3.95, N: 9.77, O: 5.70; IR (KBr): υ = 1673, 1561 cm^{-1}; ^1H NMR (DMSO-d_6, 500 MHz): δ = 1.99 (3H, s), 6.72 (1H, d, J = 8 Hz), 7.00 (1H, s), 7.21-7.35 (3H, m), 7.39 (1H, d, J = 7 Hz), 7.68 (1H, d, J = 8 Hz), 8.04 (1H, s) ppm; ^{13}C NMR (DMSO-d_6, 125 MHz): δ = 23.1, 112.9, 117.3, 117.5, 122.0, 127.6, 128.9, 129.9, 131.2, 135.1, 135.6, 139.8, 140.1, 149.7, 150.0, 158.5, 161.4 ppm; MS (70 eV): m/z = 294 (M^+).

Conclusions

In summary, we have introduced an unprecedented Pd catalyzed intramolecular cyclization of quinazolones for the facile construction of fused tetracyclic heteroarenes. A novel and efficient Pd-containing PEI phosphinite modified magnetite core-shell, Pd@Ph_2PO-PEI-mSiO_2, has been developed as highly active and stable Pd@Ph_2PO-PEI-mSiO_2 for intramolecular coupling/cyclization reactions. The PEI functionality showed good performance for raising water compatibility and acted as the base in reaction. The results show that all the reaction of different substrate containing a broad substrate scope have been proceeded well under mild conditions to give the desired products in good to high yields. The salient features of the proposed method include high efficiency, generality and simplicity which lead to high yields, a cleaner reaction profile and easy recyclability of the highly stable heterogeneous catalyst by a simple magnet separation.

Notes and references

1 (a) CH. Jun, *Chem. Soc. Rev.* 2004, **33**, 610; (b) P. Braunstein. D. Matt, D. Nobel, *Chem. Rev.* 1988, **88**, 747; (c) F. Chen, T. Wang, N. Jiao, *Chem. Rev.* 2014, **114**, 8613; (d) D. A. Petrone, J. Ye, M. Lautens, *Chem. Rev.* 2016, **116**, 8003.

2 (a) M. J. da Silva, L. Berlini, *New J. Chem.* 2016, **40**, 7996; (b) P. Ruiz-Castillo, S. L. Buchwald, *Chem. Rev.* 2016, **116**, 12564; (c) R. Hua, M. Tanaka, *New J. Chem.* 2001, **25**, 179; (d) G. Hu, J. Wang, Z. Li, Y. Liu, P. Gong, *New J.Chem.* 2018, doi: 10.1039/C7NJ04342B.

3 (a) E. M. Beccalli, G. Broggini, M. Martinelli, S. Sottocornola, *Chem. Rev.* 2007, **107**, 5318; (b) Z. Lian, B. N. Bhawal, P. Yu, B. Morandi, *Science*, 2017, **356**, 1059; (c) R. Andres, de Jesus, J. C. Flores, *New J. Chem.* 2007, **31**, 1161.

4 (a) D. Zhang, Q. Wang, *Coord. Chem. Rev.* 2015, **286**, 1; (b) C. Shen, R. R. Liu, R. J. Fan, Y. L. Li, T. F. Xu, J. R. Gao, Y. X. Jia, *J. Am. Chem. Soc.* 2015, **137**, 4936; (c) G. Zou, W. Huang, Y. Xiao, J. Tang, *New J. Chem.* 2006, **30**, 803; (d) G. Yue, K. Lei, H. Hirao, J. S. Zhou, *Angew. Chem.* 2015, **127**, 6631.

5 J. Wang, S. Tang, Q. Zhu, *Org. Lett,* 2016, **18**, 3074.

6 A. M. Signori, E. Latocheski, B. L. Albuquerque, D. Faggion, T. B. Bisol, L. Meier, J. B. Domingos, *New J. Chem.* 2015, **39**, 1574.

7 J. K. Ray, S. Paul, P. Ray, R. Singha, D. Y. Rao, S. Nandi, A. Anoop, *New J. Chem.* 2017, **41**, 278.

8 a) A. Balanta, C. Godard, C. Claver, *Chem. Soc. Rev.* 2011, **40**, 4973; b) C. Burda, X. Chen, R. Narayanan, M. A. El-Sayed, *Chem. Rev.* 2005, **105**, 1025; c) D. Astruc, *Tetrahedron: Asymmetry*, 2010, **21**, 1041; d) L. Ma'mani, A. Heydari, M. Sheykhan, *Appl. Catal. A: General,* 2010, **384**, 122.

9 a) L. Yin, J. Liebscher, *Chem. Rev.* 2007, **107**, 133; b) S. Shylesh, V. Schnemann, W. R. Thiel, *Angew. Chem.,* 2010, **122**, 3504; c) D. Astruc, E. Boisselier, C. Ornelas, *Chem. Rev.* 2010, **110**, 1857.

10 a) A. Martin, R. A. Garcia, D. SenKaraman, J. M. Rosenholm, *J. Mater. Sci.,* 2014, **49**, 1437; b) R. Sanz, G. Calleja, A. Arencibia, E. S. Sanz-Perez, *Appl. Surf. Sci.,* 2010, **256**, 5323; c) J. M. Rosenholm, A. Penninkangas, M. Linden, *Chem. Commun.,* 2006, 3909; d) E. P. Dillon, C. A. Crouse, A. R. Barron, *ACS Nano*, 2008, **2**, 156; e) L. Lou, K. Yu, Z. Zhang, R. Huang, Y. Wang, A. R. Zhu, *Appl. Surf. Sci.,* 2012, **258**, 8521; f) S. B. Khalili, A. R. Sardarian, *Monatsh Chem.,* 2012, **143**. 841.

11 X. Chen, Y. Du, H. Sun, F. Wang, L. Kong, M. Sun, *Bioorg. Med. Chem. Lett.* 2014, **24**, 884.

12 I, Khan, A, Ibrar, N. Abbas, A. Saeed, *Eur. J. Med. Chem.* 2014, **76**, 193.

13 V. G. Ugale, S. B. Bari, *Eur. J. Med. Chem.* 2014, **80**, 447.

14 C. Balakumar, P. Lamba, D. P. Kishore, B. L. Narayana, K. V. Rao, K. Rajwinder, A. R. Rao, V. Shireesha, B. Narsaiah, *Eur. J. Med. Chem.* 2010, **45**, 4904.

15 S. Hu, G. Xie, D. X. Zhang, C. Davis, W. Long, Y. Hu, F. Wang, X. Kang, F. Tan, L. Ding, Y. Wang, *Bioorg. Med. Chem. Lett.* 2012, **22**, 6301.

16 K. W. Fowler, D. Huang, E. A. Kesicki, H. C. Ooi, A. Oliver, F. Ruan, J. Treiberg, K. D. Puri, US Patent RE44599, 2013.

17 a) B. D. Krane, M. Shamma, *J. Nat. Prod.* 1982, **45**, 377; b) V. A. Glushkov, Y. V. Shklyaev, *Chem. Heterocycl. Compd.* 2001, **37** 663; c) G. R. Pettit, Y. H. Meng, D. L. Herald, K. Graham, R. K. Pettit, D. L. Doubek, *J. Nat. Prod.* 2003, **66**. 1065; d) J. H. Rigby, U. Maharoof, M. E. Mateo, *J. Am. Chem. Soc.* 2000, **122**, 6624; e) T. Hudlicky, U. Rinner, D. Gonzalez, H. Akgun, S. Schilling, P. Siengalewicz, T. A. Martinot, G. R. Pettit, *J. Org. Chem.* 2002, **67**, 8726; (f) R. Adepu, B. Prasad, M. A. Ashfaq, N. Z. Ehtesham, M. Pal, *RSC Adv.* 2014, **4**, 49324.

18 F. Coelho, D. Veronese, E. Lopes, R. C. Rossi, *Tetrahedron Lett.* 2003, **44**, 5731.

19 A. Saeed, Z. Ashraf, *Pharm. Chem. J.* 2008, **42**, 277; b) J. F. Guastavino, S. M. Barolo, R. A. Rossi, *Eur. J. Org. Chem.* 2006, **17**, 3898.

20 K. B. Simonsen, J. Kehler, K. Juhl, N. Khanzhin, S. M. Nielsen, Patent, WO2008131779A1, 2008.

21 Y. H. Wong, M. Ho, Y. Q. Hu, X. He, H. Pang, Patent, WO2008092292A1, 2008.

22 O. Plettenburg, K. Lorenz, J. Goerlitzer, M. Loehn, Patent, WO2008077555A2,. 2008.

23 Y. Asano, S. Kitamura, T. Ohra, F. Itoh, M. Kajino, T. Tamura, M. Kaneko, S. Ikeda, H. Igata, T. Kawamoto, S. Sogabe, S. Matsumoto, T. Tanaka, M. Yamaguchi, H. Kimura, S. Fukumoto, *Bioorg. Med. Chem.* 2008, **16**, 4699.

24 T. Matsui, T. Sugiura, H. Nakui, S. Iguch, S. Shigeoka, H. Tukedu, T. Odagaki, Y. Ushio. K. Ohmoto, M. Iwamani, S. Yamazaki, T. Arai, M. Kawamura, *J. Med. Chem.* 1992, **35**, 3307.

25 S. W. Li, M. G. Nair, D. M. Edwards, R. L. Kisluick, Y. Gaument, L. K. Dev, D. S. Duch, J. Humphreys, G. K. Smith, R. Ferone, *J. Med. Chem.* 1991, **34**, :2746.

26 a) M. Mahdavi, M. Bialam, M. Saeedi, F. Jafarpour, A. Foroumadi, A. Shafiee, *Synlett*, 2015, **26**, 173; (b) A. Rayatzadeh, M. Saeedi, M. Mahdavi, Z. Rezaei, R. Sabourian, M. H. Mosslemin, T. Akbarzadeh, A. Foroumadi, A. Shafiee, *Monatsh. Chem.* 2015, **146**, 637; (c) M. Asadi, M. Ebrahimi, M. Mahdavi, M. Saeedi, P. R. Ranjbar, F. Yazdani, A. Shafiee, A. Foroumadi. *Synth. Commun.* 2013, **43**, 2385; (d) M. Mahdavi, M. Bialam, M. Saeedi, F. Jafarpour, A. Foroumadi, A. Shafiee, *Synlett*, 2015, **26**, 173.

27 L. Ma'mani, S. Miri, M. Mahdavi, S. Bahadorikhalili, E. Lotfi, A. Foroumadi, A. Shafiee, *RSC Adv.* 2014, **4**, 48613; (b) G. Rahimzadeh, S. Bahadorikhalili, E. Kianmehr, M. Mahdavi, *Molec. Divers.* 2017, **21**, 597; (c) S. Bahadorikhalili, L. Ma'mani, H. Mahdavi, A. Shafiee, *RSC Adv.* 2015, **5**, 71297; (d) M. Mohammad, H. Lijan, S. Bahadorikhalili, L. Ma'mani, P. R. Rashidi, A. Shafiee, *RSC Adv.* 2016, **6**, 28838; (e) S. Bahadorikhalili, L. Ma'mani, H. Mahdavi, A. Shafiee, *Microporous Mesoporous Mater.* 2018, **262**, 207-216; (f) H. Mahdavi, O. Rahmani, *Catal. Lett.* 2016, **146**, 2292; (g) H. Mahdavi, R. Sahraei, *Catal. Lett.* 2016, **146**, 977.

View Article Online
DOI: 10.1039/C7NJ04837H

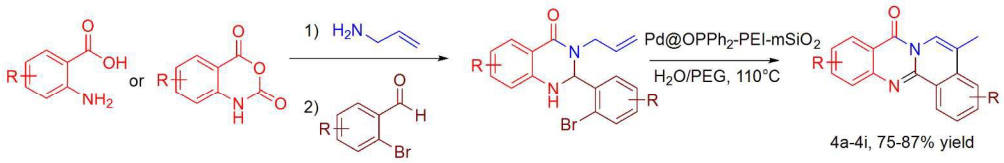

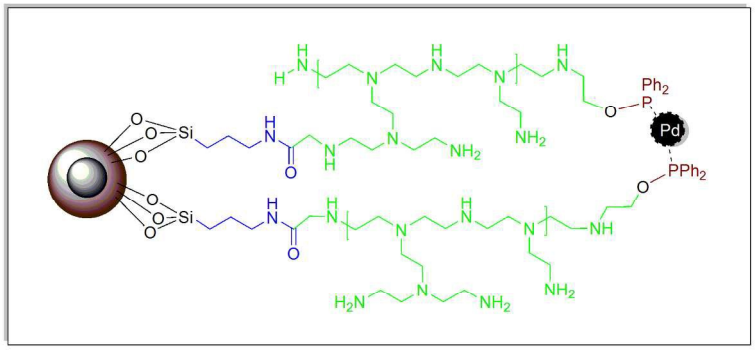

$Pd@OPPh_2$-PEI-$mSiO_2$

Graphical Abstract

188x105mm (300 x 300 DPI)